

# Voltage Controlled Oscillators for Quantum Sensing <sup>†</sup>

Reza Tavakoli Dinani <sup>1,2</sup> and Milos Nesladek <sup>1,2,\*</sup>

<sup>1</sup> IMOMECE Division, IMEC, Wetenschapspark 1, B-3590 Dipenbeed, Belgium;  
reza.tavakolidinani@uhasselt.be

<sup>2</sup> Institute for Material Research (IMO), Hasselt University, Wetenschapspark 1, B-3590 Dipenbeed, Belgium

\* Correspondence: milos.nesladek@imec.be

<sup>†</sup> Presented at the 4th International Electronic Conference on Applied Sciences, 27 October–10 November 2023; Available online: <https://asec2023.sciforum.net/>.

**Abstract:** Nitrogen vacancy defect centers are promising platform for quantum sensing. They have attracted attention over the last 15 years. Their performance has been demonstrated in laboratory scale using expensive and bulky laser and microwave sources. We report using off the shelf voltage controlled oscillators as a reliable replacement of microwave sources. They are cheap, small and consume low power. In combination with RF mixers, we tune them to drive double quantum (DQ) resonances and compensate effect of thermal drifts on NV-based magnetometer's performance by more than one order of magnitude.

**Keywords:** quantum sensing; NV defect centers; voltage controlled oscillators; double quantum resonance; feedback

## 1. Introduction

Defect centers in solid-state materials have opened a new era in quantum sensing and computing. In particular, Nitrogen-vacancy (NV) defect centers in diamond have attracted lot of attentions over the last 15 years. Their physical and chemical properties made them suitable platform for sensing. They can sense not only one but multiple parameters like magnetic field B, electric field E, pressure P, Stress M and temperature T. As a magnetic sensor they can be used as both scalar and vector magnetometers. They can operate in harsh conditions like extreme temperature, high pressure and high radiation like in space applications. They can operate at a wide range of magnetic fields. Their non-toxicity allows one to use them in biological applications. Due to their atomic-scale defect, they have provided us with high spatial resolution, which is the highest spatial resolution among magnetic sensors. They can be used as MW spectral analyzer. In addition to all these features, initialization NV based sensors with visible green light that can be provided with cheap green laser diodes.

The performance of NV centers as a reliable quantum sensor has been demonstrated in laboratory scale using expensive and bulky MW and laser sources. But it limits the applications of these magnetometers to laboratory scale ones. There are ongoing efforts to make them portable and miniaturize them so that one can exploit their features in industry, medicine, technology, military and civil applications. MW source is a key part of NV sensors that need be integrated into the sensor module. This integration should happen with minimum effect on the overall performance of the sensor. So far, to generate accurate and stable MW fields for NV based magnetometers, one typically uses the state of art MW generators. Voltage controlled oscillators (VCO), that operate in MW frequency range, are good candidates to replace bulky MW generators. VCOs are cheap, small, portable, consume low power, easy to use and available in different operating frequency ranges. Their performance as MW source for deriving NV transitions has been demonstrated. Here we would like to demonstrate VCOs capability to exclude the effect of the

**Citation:** Dinani, R.T.; Nesladek, M. Voltage Controlled Oscillators for Quantum Sensing. *Eng. Proc.* **2023**, *52*, x. <https://doi.org/10.3390/xxxxx>

Academic Editor(s): Name

Published: date



**Copyright:** © 2023 by the authors. Submitted for possible open access publication under the terms and conditions of the Creative Commons Attribution (CC BY) license (<https://creativecommons.org/licenses/by/4.0/>).

temperature drift in NV magnetic sensors. This will have potential application for NV magnetometers in space where large temperature variations happen.

## 2. Materials and Methods

NV defect centers in diamond can exist in three different charge states,  $NV_0$ ,  $NV_+$  and  $NV_-$ . Among them,  $NV_-$  shows promising platform for sensing. It has total electron spin of 1 so it has a triplet ground state with electron spin quantum numbers of  $m_s = \pm 1$  and 0. At room temperature and zero magnetic field,  $m_s = \pm 1$  is separated from  $m_s = 0$  by a zero-field-splitting (ZFS) parameter  $D = 2.87$  GHz. All three states are occupied with same probability. To optically pump ground states, one can use green laser light with wavelength of 520–532 nm. Green light excites triplet ground states to triplet excited states where they decay back to the ground states through emitting red photoluminescence light (PL). For excited state with  $m_s = \pm 1$  there is another way to get back to all ground states. This is called spin-state-dependent inter-system crossing (ISC) which is a non-radiative decay path. Consequently, the probability of having an electron spin in ground state with  $m_s = 0$  state is more likely than  $m_s = \pm 1$ . One can use MW field (in continuous or pulsed mode) to drive transitions between ground states. Changes in the electron spin population at excited states can be monitored through detecting the emitted visible red PL at a wavelength of 637 nm. And by sweeping the frequency of the MW field, one can reveal what is called optically detected magnetic resonance (ODMR) profiles. These profiles are typically follow a Lorentzian function of MW frequency. The center frequency  $f_c$  of ODMR profiles can vary by the magnetic field. By monitoring the center frequency one can determine the applied magnetic field through

$$B = 2\pi(f_c - f_{ZFS})/\gamma_e, \quad (1)$$

where  $\gamma_e = 28$  GHz/T is the gyromagnetic ratio of the electron spin. ZFS parameter  $D$  varies with temperature with a rate of  $dD/dT = -74$  kHz/K. It affects ODMR profiles corresponding to  $m_s = 0 \rightarrow -1$  and  $m_s = 0 \rightarrow +1$  transitions in the same way. To exclude the effect of temperature on magnetic reading, one can find the center frequency of both transitions and calculate the difference in their frequencies to exclude the effect of temperature variations. This requires periodic jumping in MW frequency from one profile to another. This causes blind time slots in data associated with each profile. A solution to this issue is addressing both transitions simultaneously using RF frequency mixers. We explain it more where we describe double-quantum configuration.

### 2.1. Experimental Setup

Our experimental setup has two parts, optical and electrical. In optical part we mainly initialize the electron spin state with green laser light and collect red PL. The electrical part mainly includes, VCO to drive electron spin state transitions, photodetector to detect PL and lock-in amplifier to analyze modulated PL signal.

Our  $NV_-$ -based magnetometer is installed on an optical table. We used a 80 mW laser diode as the laser source to initialize the sensor. The LD operates in constant current mode and it was controlled by a laser diode driver kit. Its temperature also was under control using a thermo-electric control (TEC) unit. An objective is used to focus the laser light on the  $NV_-$  diamond sample. The sample has a size of 3 mm × 3 mm. The same objective is used to collect red PL emitted from the sample. The collected red PL passes through a dichroic mirror to suppress green light before reaching to the 1st channel of a balanced-detection photodiode. The 2nd channel of the detector is used to monitor the green laser fluctuations. The outputs of both channels are subtracted and amplified. The diamond sample is installed on a 5 cm × 5 cm PCB. We have sputtered co-planar MW antenna on the surface of the sample to apply MW field. The antenna is wire bonded to the PCB. Advantage of using sputtered antenna is its low power consumption compared to other types of MW antenna like MW loop or MW resonator. The PCB containing the sample

is placed inside a three pairs of Helmholtz coils. The coils are used to apply magnetic field in x, y and z directions. The current of the coils are controlled by a programmed current source so that we can tune the magnitude and direction of the applied magnetic field. Figure 1 illustrates our magnetometry setup.

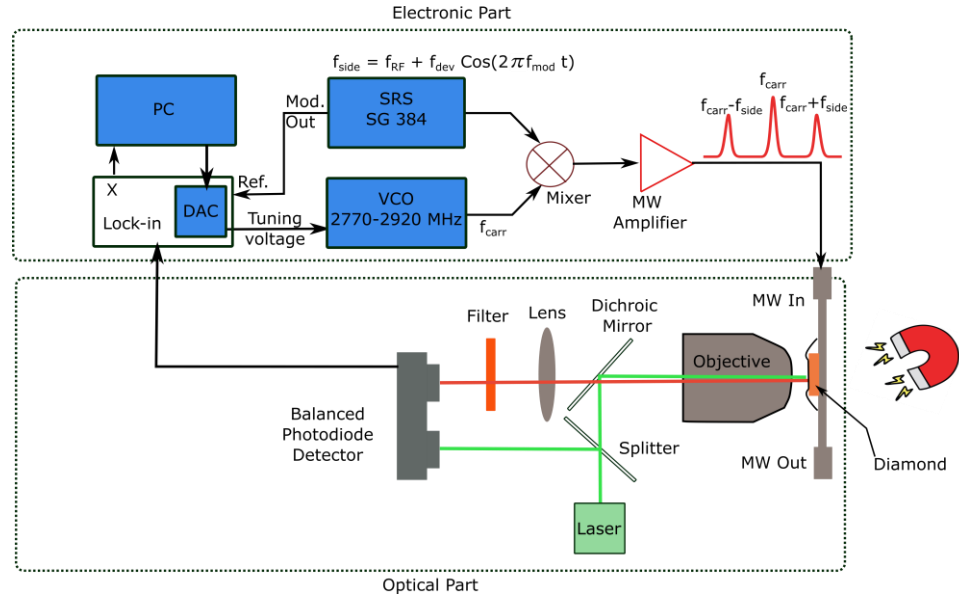


**Figure 1.** Schematic of setup used to sense magnetic field using NV- sensor. Balanced detection scheme is used to minimize the effect of the laser intensity fluctuations. MW source is designed to perform double-quantum configuration with frequency modulated signal. Temperature drift in sensor is compensated through a feedback control loop where tuning voltage of VCO is actively updated. An 18-bit DAC imbedded in the lock-in amplifier is used to apply tuning voltage of the VCO.

The scheme of the electronic part of the setup is shown in Figure 1. A VCO model CVCO-55CC 2770-2920 is used to apply a MW carrier frequency  $f_{carr}$  about ZFS parameter  $D = 2.78$  MHz. It has a nominal tuning sensitivity of 48 (MHz/V). A RF/MW source model of SRS SG384 is used to generate a frequency modulated RF signal. We call it side frequency  $f_{side}$  where it is a sinusoidal function of time,

$$f_{side} = f_{RF} + f_{dev} \cos(2\pi f_{mod} t), \quad (2)$$

where  $f_{dev}$  is called deviation frequency and  $f_{mod}$  is modulation frequency. We typically use  $f_{mod} = 10$  kHz and  $f_{dev} = 800$  kHz.  $f_{mod}$  is used as the reference frequency  $f_{ref}$  of the lock-in amplifier. The VCO supply and tuning voltages were provided with a 18-bit digital-analog-converter (DAC) imbedded into a Zurich Instrument lock-in amplifier model LMF1. The input of the amplifier comes from the output of the balanced photodiode. We typically adjust the phase of the lock-in reference to maximize the in-phase signal and leave mostly the electronic noise into the quadrature component of lock-in output. The outputs of the VCO and SRS were fed into a mixer model ZX05-73L. The mixer's output exhibits two primary frequencies at  $f_{carr} \pm f_{side}$  with opposite modulation phases. Subsequently, this output is amplified using a microwave amplifier with a nominal gain of 45 dB before being directed to the sputtered antenna.

### 2.2. Double-Quantum Configuration

To keep track of thermal drift in the sensor, we operate in double quantum (DQ) configuration where MW field is used to drive both  $m_s = 0$  to  $m_s = \pm 1$  transitions simultaneously. A simple method proposed by is depicted in Figure 1. It is based on using two MW sources and a mixer. MW sources generate  $f_{carr}$  and  $f_{side}$  where  $f_{side}$  depends on the Zeeman splitting between ground states with  $m_s = +1$  and  $m_s = -1$ . In our case this splitting is about 6.1 MHz. By choosing right value of  $f_{side}$ , one can drive resonance transitions

associated with  $m_s = 0$  to  $m_s = \pm 1$  transitions. Figure 2 shows the dispersive pattern response of the lock-in when we sweep  $f_{\text{carr}}$ . Those patterns on the left/right correspond with situation in which we drive ground states with  $m_s = 0$  to  $\pm 1$  transitions separately. These transitions are labeled as single resonance (SR) transitions. The pattern at the center corresponds with the DQ configuration. For magnetometry application, one needs to stay on the linear part of the dispersive pattern. And preferentially at zero crossing point of it. In presence of thermal fluctuations, zero crossing point will move either to the right or left. This results in fake magnetic reading and must be corrected. In our case, we actively update  $f_{\text{carr}}$  so that we can stay at or close to the zero crossing where typically maximum slope occurs. In this way we can ensure thermal drift is minimized and has no effect on the magnetic sensings. We used a proportional-integral-derivative (PID) algorithm written in Python to calculate the update value of  $f_{\text{carr}}$ . In our PID algorithm, the set point is the zero crossing and the control parameter is  $f_{\text{carr}}$ .

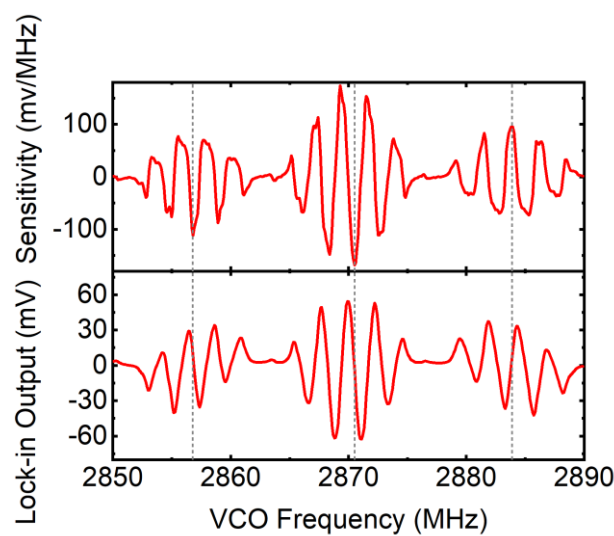


**Figure 2.** (Bottom) In-phase component of the lock-in amplifier output in response to a MW frequency modulated red PL. (Top) first order differentiate of bottom panel. Horizontal axis represents  $f_{\text{carr}}$  frequency applied by VCO. Vertical dot-lines represent where we get maximum sensitivity.  $f_{\text{carr}}$  is swept to reveal dispersive patterns associate with single (at the left and right) and double (at the center) quantum resonances.

### 3. Results and Discussion

We noticed an increment of about  $2/3$  in slope of dispersive patter under DQ configuration as it is shown in Figure 2. This is more than the expected increment of  $4/3$  which is predicted theoretically. We believe this issue is a result of suboptimal sensitivity in the SR configuration. If this is indeed the case, DQ demonstrates how we can enhance the sensitivity of the non-optimized SR configuration.

We evaluated the capability of our sensor in correcting the effect of the thermal drift on its readout. Figure 3 demonstrates the performance of our feedback control under slow and fast ambient temperature drift. In latter one, we turned on a heater to blow hot air flow to our setup. The heater was about 1 m away from the setup to have less magnetic disturbance on sensor's reading. Figure 3 shows the Allan Standard Deviation (ASD) of the in-phase component of the lock-in amplifier output in response to a frequency modulated Red PL input signal. It contains data associated with measurements with and without feedback control. Both measurements were carried out under the same experimental conditions but at different times. However, we observed the same results when repeating the measurements. One can note an order of magnitude improvement in ASD at integration time of 100 when the feedback control is active. At integration times less than about 16 sec, detection scheme without feedback provides better sensitivity. But as time goes on

sensor's output drifts, and sensor operating in feedback scheme performs better. This is due to the relatively large tuning sensitivity of the VCO that does not let us to update  $f_{\text{carr}}$  with steps finer than about 3 kHz. As ZFS parameter D varies by temperature with a rate of  $dD/dT = -74$  kHz/K. This results in a minimum control temperature step of 40 mK. To achieve a better temperature control, one can use a VCO with smaller tuning sensitivity or a voltage source with finer tuning voltage.

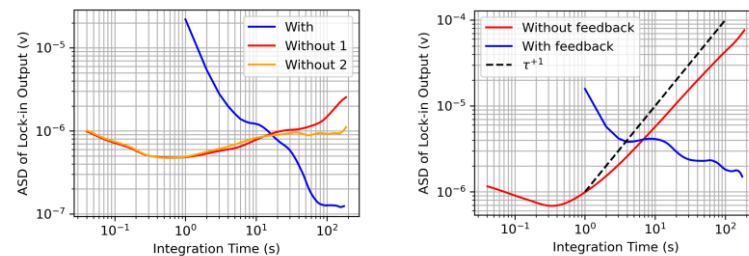


**Figure 3.** Allan standard deviation of the in-phase component of the lock-in amplifier output in response to the frequency modulated PL signal. Data were collected when background temperature drifts (left) slowly (right) fast. Each plot shows measurements with and without feedback control. Dashed line is meant as reference guide for drift effects with slope +1.

#### 4. Conclusions

We demonstrated how a VCO can be used to implement DQ sensing configuration in NV- magnetic sensor. It provides the carrier frequency around ZFS parameter. Its value can be updated actively over the course of the measurement using a PID algorithm. This excludes the effect of thermal drift in sensors readout. We observed one order of magnitude improvement in the sensor's sensitivity at integration times longer than 100 s. What we have demonstrated here can extend the dynamic range of NV- sensors operating in frequency modulated scheme and in thermally drifting environment. Even in thermally stable environment, high intensity laser light can change the temperature of the sensor.

Then an active feedback control scheme, can suppress sensor's temperature variation effect.

#### Author Contributions:

**Funding:** This research was funded by the European Union's Horizon Europe research and innovation program under grant agreement No. 101080136 (AMADEUS).

**Institutional Review Board Statement:** Not applicable.

**Informed Consent Statement:** Not applicable.

**Data Availability Statement:** Not applicable.

**Conflicts of Interest:** The authors declare no conflict of interest. The funders had no role in the design of the study; in the collection, analyses, or interpretation of data; in the writing of the manuscript; or in the decision to publish the results.

#### References

1. Degen, C.L. Scanning magnetic field microscope with a diamond single-spin sensor. *Appl. Phys. Lett.* **2008**, *92*, 14.
2. Loss, D.; DiVincenzo, D.P. Quantum computation with quantum dots. *Phys. Rev. A* **1998**, *57*, 120.
3. Childress, L.; Gurudev Dutt, M.V.; Taylor, J.M.; Zibrov, A.S.; Jelezko, F.; Wrachtrup, J.; Hemmer, P.R.; Lukin, M.D. Coherent Dynamics of Coupled Electron and Nuclear Spin Qubits in Diamond. *Science* **2006**, *314*, 281–285.
4. Sushkov, A.O.; Lovchinsky, I.; Chisholm, N.; Walsworth, R.L.; Park, H.; Lukin, M.D. Magnetic Resonance Detection of Individual Proton Spins Using Quantum Reporters. *Phys. Rev. Lett.* **2014**, *113*, 197601.
5. Doherty, M.W.; Manson, N.B.; Delaney, P.; Jelezko, F.; Wrachtrup, J.; Hollenberg, L.C. The nitrogen-vacancy colour centre in diamond. *Phys. Rep.* **2013**, *528*, 1–45.
6. Barry, J.F.; Schloss, J.M.; Bauch, E.; Turner, M.J.; Hart, C.A.; Pham, L.M.; Walsworth, R.L. Sensitivity optimization for NV-diamond magnetometry. *Rev. Mod. Phys.* **2020**, *92*, 015004.

7. Clevenson, H.; Pham, L.M.; Teale, C.; Johnson, K.; Englund, D.; Braje, D. Robust high-dynamic-range vector magnetometry with nitrogen-vacancy centers in diamond. *Appl. Phys. Lett.* **2018**, *112*, 25.
8. Wu, Y.; Jelezko, F.; Plenio, M.B.; Weil, T. Diamond Quantum Devices in Biology. *Angew. Chem. Int. Ed.* **2016**, *55*, 6586–6598.
9. Lovchinsky, I.; Sushkov, A.O.; Urbach, E.; de Leon, N.P.; Choi, S.; De Greve, K.; Evans, R.; Gertner, R.; Bersin, E.; Müller, C.; et al. Nuclear magnetic resonance detection and spectroscopy of single proteins using quantum logic. *Science* **2016**, *351*, 836–841.
10. Magaletti, S.; Mayer, L.; Roch, J.F.; Debuisschert, T. A quantum radio frequency signal analyzer based on nitrogen vacancy centers in diamond. *Commun. Eng.* **2022**, *1*, 19.
11. Barry, J.F.; Turner, M.J.; Schloss, J.M.; Glenn, D.R.; Song, Y.; Lukin, M.D.; Park, H.; Walsworth, R.L. Optical magnetic detection of single-neuron action potentials using quantum defects in diamond. *Proc. Natl. Acad. Sci. USA* **2016**, *113*, 14133–14138.
12. Stürner, F.M.; Brenneis, A.; Buck, T.; Kassel, J.; Rölver, R.; Fuchs, T.; Savitsky, A.; Suter, D.; Grimmel, J.; Hengesbach, S.; et al. Integrated and Portable Magnetometer Based on Nitrogen-Vacancy Ensembles in Diamond. *Adv. Quantum Technol.* **2021**, *4*, 2000111.
13. Webb, J.L.; Clement, J.D.; Troise, L.; Ahmadi, S.; Johansen, G.J.; Huck, A.; Andersen, U.L. Nanotesla sensitivity magnetic field sensing using a compact diamond nitrogen-vacancy magnetometer. *Appl. Phys. Lett.* **2019**, *114*, 231103.
14. Mamin, H.J.; Sherwood, M.H.; Kim, M.; Rettner, C.T.; Ohno, K.; Awschalom, D.D.; Rugar, D. Multipulse Double-Quantum Magnetometry with Near-Surface Nitrogen-Vacancy Centers. *Phys. Rev. Lett.* **2015**, *115*, 079901.
15. Goldman, M.L.; Doherty, M.W.; Sipahigil, A.; Yao, N.Y.; Bennett, S.D.; Manson, N.B.; Kubanek, A.; Lukin, M.D. State-selective intersystem crossing in nitrogen-vacancy centers. *Phys. Rev. B* **2015**, *91*, 165201.
16. Fescenko, I.; Jarmola, A.; Savukov, I.; Kehayias, P.; Smits, J.; Damron, J.; Ristoff, N.; Mosavian, N.; Acosta, V.M. Diamond magnetometer enhanced by ferrite flux concentrators. *Phys. Rev. Res.* **2020**, *2*, 023394.

**Disclaimer/Publisher's Note:** The statements, opinions and data contained in all publications are solely those of the individual author(s) and contributor(s) and not of MDPI and/or the editor(s). MDPI and/or the editor(s) disclaim responsibility for any injury to people or property resulting from any ideas, methods, instructions or products referred to in the content.